Journal of Applied Electrochemistry **31**: 1221–1226, 2001.

A study of the adsorption properties of commercial carbon dioxide corrosion inhibitor formulations

W.H. DURNIE, B.J. KINSELLA, R. DE MARCO and A. JEFFERSON
Western Australian Corrosion Research Group, School of Applied Chemistry, Curtin University of Technology, GPO Box U1987, Perth, Western Australia 6845

Received 23 August 2000; accepted in revised form 19 June 2001

Key words: adsorption isotherms, carbon dioxide corrosion, corrosion inhibitors, FTIR

Abstract

Corrosion rate data for several commercial carbon dioxide corrosion inhibitors have been fitted to the Temkin adsorption isotherm and van't Hoff equation, enabling a determination of the enthalpy of adsorption (ΔH°_{ad}). It has been found that experimentally determined ΔH°_{ad} values for commercial inhibitor formulations can provide valuable insights into the behaviour of the inherent active components. The temperature sensitivities along with the mechanism of adsorption (physi- or chemisorption) and the minimum concentration required for activity of inhibitors is determinable by this approach. Additionally, FTIR has been used to identify those inhibitors that are tenaciously adsorbed to steel, and suitable for use in batch treatment applications.

1. Introduction

Carbon dioxide corrosion is a major problem in the oil and gas production industry, and can occur at all stages of production from downhole to surface equipment and processing facilities [1]. The corrosion of wet gas and multiphase pipelines is responsible for lost production and costly repairs, necessitating a corrosion control program (e.g., organic corrosion inhibitors are used widely in the control of internal corrosion in oil and gas production/transportation [2]). The use of carbon steel in conjunction with a chemical inhibitor treatment programme is a cost-effective and preferred method for the control of carbon dioxide corrosion.

Present research is directed towards elucidation of the mechanism for carbon dioxide corrosion inhibition in order to produce highly efficacious and cost-effective corrosion inhibitors. Slight improvements in inhibitor performance can save the oil industry millions of dollars per annum in specialty chemicals. Furthermore, recent environmental concerns have led to the development of low toxicity or 'green' or 'environmentally friendly' corrosion inhibitors [3, 4].

Commercial corrosion inhibitors comprise at least one of the following surfactants: fatty acids; amines; fatty amines/diamines; fatty amido-amines or imidazolines; oxyalkylated amines; quaternary amines; other amine derivatives; and oxygen, sulfur or phosphorous containing compounds [5]. These surfactants adsorb to the steel surface, yielding a protective hydrophobic film that impedes the corrosion of steel [6].

Recent studies have attempted to construct a quantitative structure/activity relationship (QSAR) to describe the efficacy of a variety of oil field corrosion inhibitors [3, 4, 7, 8]. Despite the recent advancements in QSAR studies, the most significant selection criterion is the efficiency of the inhibitor under specific field-like conditions.

It is possible to interpret the efficacy of corrosion inhibitors by using classical adsorption isotherms [7, 9–12]. If the steel electrode is assumed to corrode uniformly then the corrosion rate in the absence of inhibitor $\{v_{corr}(\text{blank})\}$ is representative of the total number of corroding sites, while the corrosion rate in the presence of inhibitor $\{v_{corr}(\text{inhibited})\}$ is symbolic of the number of available corroding sites remaining after blockage of some sites by inhibitor adsorption [12]. The melding of these assumptions yields the fractional surface coverage (θ), namely,

$$\theta = \frac{v_{corr}(\text{blank}) - v_{corr}(\text{inhibited})}{v_{corr}(\text{blank})} \tag{1}$$

Temkin adsorption isotherm plots (i.e., $\theta/\ln C$) can be used to determine the fundamental adsorption properties of commercial corrosion inhibitors [7], that is,

$$K_{ad}C = e^{f\theta} \text{ and } \theta = \left(1/f\right)\ln K_{ad} + \left(1/f\right)\ln C \tag{2}$$

where K_{ad} is the adsorption equilibrium constant, f the molecular interaction constant, and C is the analytical

concentration of the inhibitor solution expressed in units of mol kg^{-1}.

Isosteric enthalpies of adsorption (i.e., ΔH°_{ad}) are obtained by constructing van't Hoff plots of $\ln C_{\theta=0.5}$ against $1/T$ over a suitable temperature range (30–70 °C), namely,

$$\ln C_{\theta=0.5} = \frac{\Delta H^{\circ}_{ad}}{RT} + \text{constant} \quad (3)$$

where $C_{\theta=0.5}$ corresponds to the concentration of inhibitor required for $\theta = 0.5$.

A detailed understanding of the mechanism of adsorption for corrosion inhibitors requires the characterisation of corrosion inhibitor films by using surface analytical techniques such as surface enhanced Raman spectroscopy (SERS), X-ray photoelectron spectroscopy (XPS), Fourier transform infrared (FTIR) spectroscopy, etc. [16, 18–22].

The present study used adsorption isotherms [7] in studies of the efficacy of commercial carbon dioxide corrosion inhibitors. This approach, which is capable of determining temperature sensitivities for commercial inhibitor products, is extremely useful as it provides a laboratory-based method for assessing the suitability of inhibitors to be used under specific oil field conditions. Furthermore, the determined ΔH°_{ad} values are indicative of the mechanism of adsorption of the inhibitors (physi- or chemisorption), establishing if a commercial product is suitable for use in continuous injection or batch treatment applications. Finally, grazing incidence FTIR has been used to corroborate if commercial inhibitors are physi- or chemisorbed to steel, verifying their suitability for use in continuous injection or batch applications.

2. Experimental details

2.1. *Electrochemical measurements*

A standard three-electrode cell comprising a mild steel (SAE/AISI Grade 1022 according to AS 1443) rotating cylinder working electrode (diameter 1.21 cm, height 0.773 cm and area 2.94 cm^2, yielding a wall sheer stress of 1 N m^{-2} at 1000 rpm [23]) and a double junction silver–silver chloride reference electrode, along with a platinum mesh auxiliary electrode, was utilized in all electrochemical measurements. A 3% (w/v) sodium chloride solution containing 100 mg L^{-1} sodium bicarbonate (AR) in milli-Q water was used as the electrolyte. The electrolyte was saturated with carbon dioxide at atmospheric pressure by continuously purging with carbon dioxide at a flow rate of approximately 200 mL min^{-1}. The working electrode was rotated at a speed of 1000 rpm during all electrochemical measurements.

The electrochemical cell was connected to a computer controlled potentiostat/galvanostat (ACM Gill 12 *DSP*) which was operated by software supplied by ACM instruments. Linear polarization (LP) measurements were conducted to determine corrosion rates at the mild steel electrodes. Corrosion rates in the presence of inhibitors can be calculated by using surface coverage data in conjunction with Equation 1 and mean blank corrosion rates for mild steel electrodes of 1.84 ± 0.18 mm y^{-1} at 30 °C, 3.24 ± 0.35 mm y^{-1} at 50 °C, and 5.10 ± 0.70 mm y^{-1} at 70 °C.

2.2. *Surface analysis*

Coupons were polished mechanically using 320, 400, 600, 800 and 1200 grit emery paper in conjunction with an ethanol lubricant. The coupons were cleaned, degreased in ethanol, and precorroded in the electrolyte for 1.5 h. The temperature was maintained at 50 °C by using an Activon 720 series digital hot plate (Barnstead/Thermolyne, Iowa USA). After a precorrosion that allowed for the formation of a corrosion product scale, the coupons were immersed in the supplied corrosion inhibitor solutions that comprised 10–30% of active ingredients. After 15 min of filming, the coupons were returned to the electrolyte for a further hour, simulating a wash step, or exposure to uninhibited produced fluids.

Coupons were removed from solution, washed in a small amount of ethanol, and dried under a stream of carbon dioxide. Coupons were stored in a vacuum desiccator until surface analyses were undertaken.

2.3. *Infrared analysis*

Infrared spectra were recorded using a Bruker IFS 66 spectrometer. The spectra of inhibitors adsorbed onto steel coupons were recorded by using a polarized grazing angle attachment and both s- and p-polarization, and 256 scans were accumulated using a resolution of 4 cm^{-1}, a 40 kHz scanner velocity, and an aperture of 4–7 mm (depending on the polarization used). The significance of the polarizer has been discussed elsewhere [24].

3. Results and discussion

3.1. *Adsorption isotherms*

A Temkin adsorption isotherm plot for an unspecified proprietary blend of two inhibitors (i.e., inhibitor D) is presented in Figure 1, and corresponding van't Hoff plots for commercial and noncommercial inhibitors are presented in Figure 2. Note, the large change in θ of 0.2–0.8 for such a narrow concentration window of 9×10^{-6}–1.4×10^{-5} g L^{-1} (Figure 1) is symbolic of a highly efficacious corrosion inhibitor with a large adsorption equilibrium constant and correspondingly high levels of corrosion protection at low inhibitor

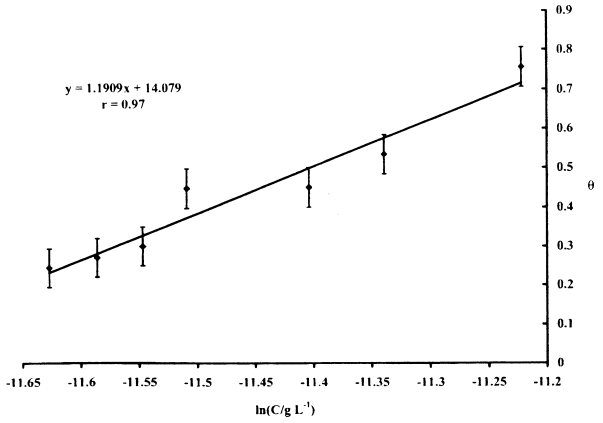

Fig. 1. Temkin adsorption isotherm–inhibitor D (unspecified blend of two inhibitors) at 30 °C.

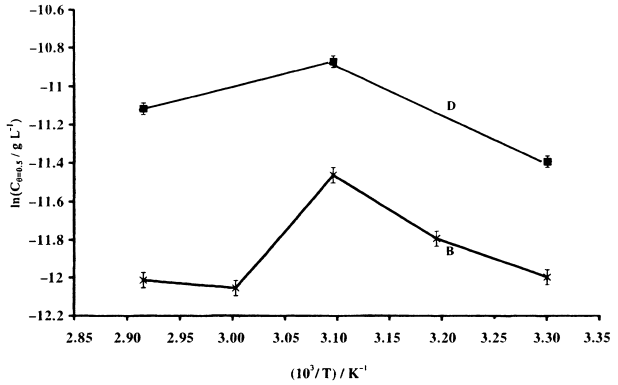

Fig. 2. Van't Hoff plots for selected inhibitors between 30–70 °C: (A) fatty acid amine; (C) imidazoline/ester; (E) amine based fatty acid; (F) quaternary amine; mercaptan; and cetylamine.

dosages. Furthermore, the errors in θ in Figure 1 were determined using an average standard error for replicate measurements in this and a previous study [7].

Although the molar masses of inhibitor active ingredients were unknown, all had similar recommended dosing levels. This lack of information does not impact on the enthalpies of adsorption, as the slopes of van't Hoff plots (equivalent to $\Delta H^{\circ}_{ad}/R$) are independent of the concentration units, that is, $\ln(C/\text{molal}) = \Delta H^{\circ}_{ad}/RT + \text{constant}$, but if C/g L^{-1} is substituted in place of C/molal then we obtain

$$\ln(C/\text{g L}^{-1}) = \frac{\Delta H^{\circ}_{ad}}{RT} + \text{constant} - \ln K \qquad (4)$$

where K is the constant conversion factor from g L^{-1} to molality which incorporates the molar mass of the inhibitor. Simply, the use of C/g L^{-1} causes a van't Hoff plot to slide up or down the y axis without altering the slope and the value of ΔH°_{ad}.

3.2. *Fundamental adsorption properties*

The van't Hoff plots in Figure 2 convey the temperature sensitivities for commercial inhibitor formulations and

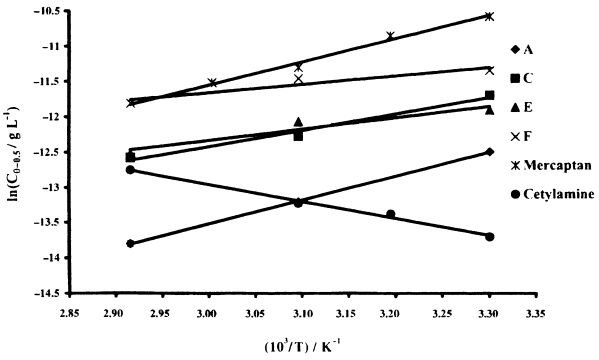

Fig. 3. Van't Hoff plots for inhibitors B and D (unspecified proprietary blends of two inhibitors).

two pure inhibitor compounds. The errors for ln $C_{\theta=0.5}$ in Figures 2 and 3 were determined graphically by using lines of minimum and maximum slopes for the corresponding adsorption isotherms at each temperature. Formulations B and D comprising unspecified proprietary blends of two inhibitors are not shown in Figure 2 as they did not display the classical van't Hoff behaviour (i.e., linearity of ln C against $1/T$), and are presented separately in Figure 3 which reveal the performance of these compounds changes with temperature, but unlike the other products, the performance diminishes with increasing temperature up to 50 °C, after which an improvement is noted up to 70 °C. Respectively, this behaviour is indeed consistent with the presence of two corrosion inhibitors possessing exothermic and endothermic enhalpies of adsorption. In this case, one component 'dominates' because of its large exothermic adsorption enthalpy over 30–50 °C, but between 50–70 °C, the other inhibitor possessing a dominant endothermic enthalpy of adsorption displays a higher level of activity. For example, if the testing of products B and D were conducted at a single temperature of 50 °C then these inhibitors would be performing at well below their optimum, emphasizing the importance of using adsorption thermodynamic studies in the characterisation of commercial inhibitor formulations. Most of the commercial products used in this study yielded a positive slope corresponding to an endothermic adsorption process, signifying a chemisorption mechanism and the suitability of these inhibitors for batch treatment applications [7]. Other compounds such as cetylamine (Figure 2), undergo an exothermic physisorption process [7], whereby performance diminishes at elevated temperature, indicating that products of this type are unsuitable in high temperature applications.

Figure 2 also shows that the fatty acid amine inhibitor (i.e., formulation A) displayed the best performance, as evident by lower values of ln $C_{\theta=0.5}$ compared to the other inhibitors. The imidazoline/ester (i.e., formulation C) and amine based fatty acid (i.e., formulation E) inhibitors performed comparably over the temperature range, while the quaternary amine (i.e., formulation F) inhibitor exhibited a degraded performance compared

Table 1. Summary of the enthalpy of adsorption data: (A) fatty acid amine, (B) unspecified proprietary blend of two inhibitors, (C) imidazoline/ester, (D) unspecified proprietary blend of two inhibitors, (E) amine based fatty acid and (F) quaternary amine

Product	ΔH°_{ad}/kJ mol^{-1}
A	+28.3 ± 1.6
B	Multiple active ingredients
C	+19.1 ± 0.8
D	Multiple active ingredients
E	+13.2 ± 1.8
F	+9.9 ± 1.9

to formulations A, C and E, but generally outperformed products B and D (compare Figures 2 and 3).

Table 1 summarizes the enthalpies of adsorption for the commercial corrosion inhibitors. Due to the non-linear behaviour of products B and D arising from the presence of multiple active ingredients, ΔH°_{ad} values could not be assigned to these inhibitors.

The concentrations required for greater than 90% protection for the six inhibitors at 30, 50 and 70 °C are also shown in Table 2; all the products reached this high level of protection at $\leqslant$5 ppm. Evidently, the dosing of corrosion inhibitors at optimum levels provides a significant saving to oil producers who commonly use arbitrarily chosen concentrations which can be orders of magnitude higher than the required level.

3.3. *Surface analysis*

Grazing incidence FTIR was conducted on coupons exposed to all of the commercial inhibitor formulations. Only two of the inhibitors (i.e., fatty acid amine inhibitor A and imidazoline/ester inhibitor C) were detected on the surface by using *ex situ* grazing angle FTIR and s-polarization (radiation polarized in a plane parallel to the sample surface).

Table 2. Summary of the concentrations of inhibitor required for high levels of protection. Inhibitors A–E have been defined in Table 1

Inhibitor	Temperature/°C	Concentration to give ~ 90% protection/ppm
A	30	1.3–1.4
A	50	1.1–1.2
A	70	0.7–0.8
B	30	2.6–2.8
B	50	3.8–4.0
B	70	2.2–2.4
C	30	2.8–3.0
C	50	1.6–1.8
C	70	1.2–1.3
D	30	3.6–3.8
D	50	5.4–5.6
D	70	4.4–4.6
E	30	2.3–2.5
E	50	2.1–2.3
E	70	1.5–1.7
F	30	3.7–3.9
F	50	3.6–3.8
F	70	2.8–3.0

The absence of signals for the other products is due to the *ex situ* nature of grazing incidence FTIR which involves the washing of treated specimens to remove all but the most tenaciously chemisorbed inhibitors. Figure 4 shows the FTIR spectrum of the neat inhibitor A, while Figure 5 shows the spectrum obtained from the surface of the coupon exposed to inhibitor A. It can be seen that both spectra possess several matching peaks; namely, those due to the hydrocarbon moiety of the inhibitor, ν_{as} CH_3 (2962 cm^{-1}), ν_{as} CH_2 (2930 cm^{-1}), ν_s CH_3 (2870 cm^{-1} barely visible), ν_s CH_2 (2853 cm^{-1}), and δ_{as} CH_3 (1462 cm^{-1}) [25], along with other bands which are assignable to the polar head group of the inhibitor molecule (i.e., the fatty acid amine functional groups).

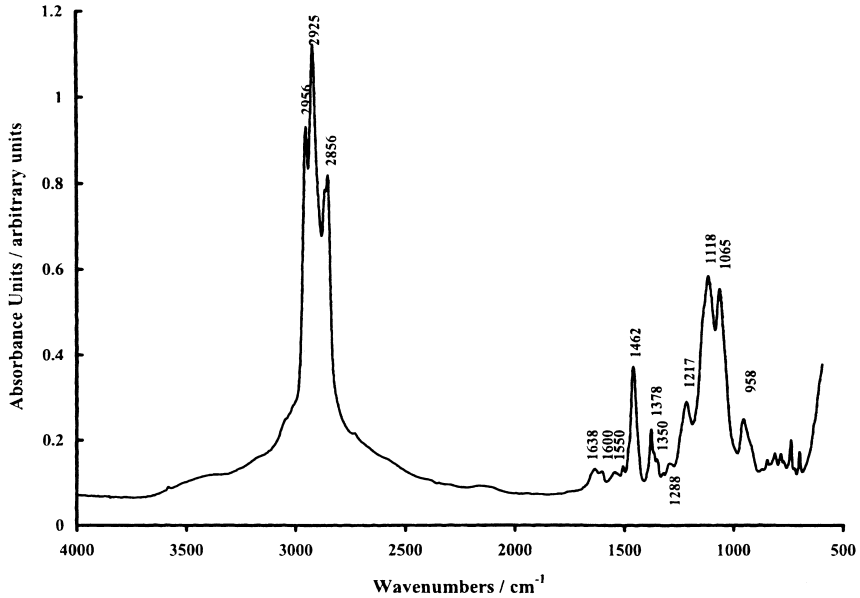

Fig. 4. FTIR spectrum of neat inhibitor formulation A (fatty acid amine).

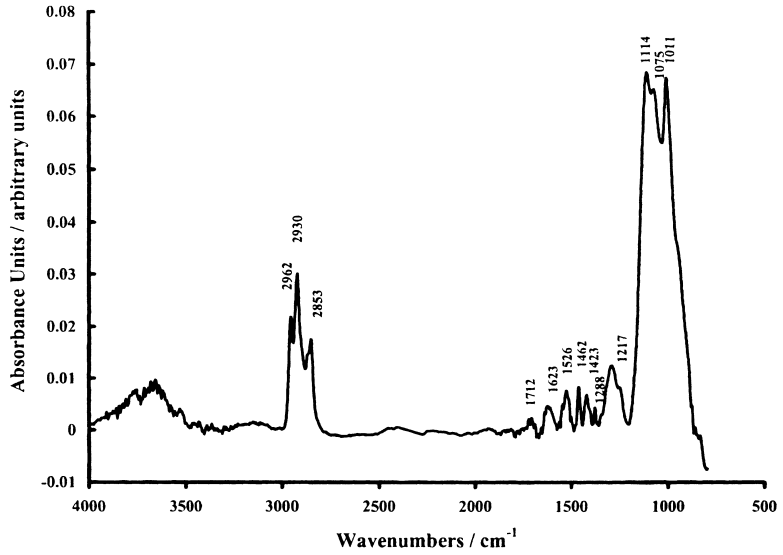

Fig. 5. s-polarized FTIR spectrum obtained from coupon exposed to inhibitor A (fatty acid amine).

Although the exact structure of this fatty acid amine inhibitor is unknown, some qualitative observations can be made. The weak broad peaks around 3500–3310 cm^{-1} in Figures 4 and 5 are attributable to the weak ν_{N-H} of the primary or secondary amine and/or an amide functional groups in this fatty acid amine-based inhibitor. The broad humps between 3000–2500 cm^{-1} are indicative of the carboxylic acid functionality in this fatty acid amine inhibitor; however, there are no discernible carbonyl peaks in the 1750 cm^{-1} region of the spectrum. As expected for a fatty acid amine-based inhibitor, the appearance of peaks at 1526 and 1423 cm^{-1} in the spectrum for the adsorbed inhibitor (Figure 5) are symbolic of an inorganic carboxylate salt such as iron(II)-carboxylate [25]. The peak at 1462 cm^{-1} in both spectra is probably due to the δ_{as} CH_3, possibly with a contribution from the CH_2 scissor on the high wavenumber side of the 1462 cm^{-1} peak, while the peak at 1378 cm^{-1} in both spectra could be due to δ_s CH_3. The spectrum of the neat formulation and the adsorbed species comprise several common peaks between 1011–1118 cm^{-1} that are probably due to C–N and/or C–O stretching in the fatty acid amine inhibitor [25]. Although some of the peaks cannot be conclusively assigned to a particular functional group, it must be noted that the concentration of active constituents comprises less than 10% of the formulation, and many other organic compounds (solvents, demulsifiers etc.) represent the balance. Note, the FTIR spectra for inhibitor C (viz., imadazoline/ester) are not shown due to their similarity to those for inhibitor A (i.e., fatty acid amine).

4. Conclusions

The concentrations for optimum levels of corrosion protection for six commercial inhibitors are shown to be $\leqslant 5$ ppm under the given test conditions encompassing a temperature range of 30–70 °C.

Ex situ surface analyses by using grazing angle FTIR can be used to elucidate the mechanism of adsorption for commercial corrosion inhibitors at corroding steel surfaces (i.e., differentiate between physi- or chemisorption). If an inhibitor undergoes chemisorption then it is suitable for use in batch treatment applications. Significantly, this spectroscopic information is valuable to the end users of the inhibitors (i.e., oil producers).

Acknowledgements

The authors thank the Australian Research Council for a Small Grant. WHD thanks the Australian Research Council for an Australian Postgraduate Award (Industry) Scholarship, along with the Western Australian Corrosion Research Group for supplementary financial support.

References

1. S.L. Fu, J.G. Garcia and A.M. Griffin, Corrosion'96, Paper 21, NACE International (1996).
2. S. Webster, D. Harrop, A.J. McMahon and G.J. Partidge, Corrosion'93, Paper 109, NACE International (1993).
3. W.P. Singh, J. Ahmed, G.H. Lin, Y. Kang and J.O.'M. Bockris, Corrosion'95, Paper 33, NACE International (1995).
4. W.P. Singh, G. Lin, J.O.M. Bockris and Y. Kang, Corrosion'98, Paper 208 (1998).
5. J.E. Donham, 'Chemical Inhibitors for Corrosion Control', Vol. 71, Royal Society of Chemistry, Great Britain (1990), p. 21.
6. E. Schaschl, *in* C.C. Nathan (Ed.), 'Corrosion Inhibitors', NACE, Houston (1981), p. 28.
7. W.H. Durnie, R. De Marco, B.J. Kinsella and A. Jefferson, *J. Electrochem. Soc.* **146** (1999) 1751.
8. V.S. Sastri and J.R. Perumareddi, *Corrosion* **50** (1994) 432.
9. Z. Szklarska-Smialowska and G. Wieczorek, *Corros. Sci.* **11** (1971) 843.
10. Z. Szklarska-Smialowska, *NATO ASI Ser.*, Ser. E. **203** (1991) 545.
11. S.L. Granese, *Corrosion* **44** (1988) 322.
12. B.B. Damaskin, O.A. Petrii and V.V. Batrakov, 'Adsorption of Organic Compounds on Electrodes' (Plenum Press, New York, 1971).

13. L.J. Simpson and C.A. Melendres, *J. Electrochem. Soc.* **143** (1996) 2146.
14. J. Uehara and K. Aramaki, *J. Electrochem. Soc.* **138** (1991) 3245.
15. J. Uehara, H. Nishihara and K. Aramaki, *J. Electrochem. Soc.* **137** (1990) 2677.
16. K. Aramaki and J. Uehara, *J. Electrochem. Soc.* **136** (1989) 1299.
17. N. Ohno, J. Uehara and K. Aramaki, *J. Electrochem. Soc.* **140** (1993) 2512.
18. G. Banerjee and S.N. Malhotra, *Corrosion* **48** (1992) 10.
19. P.F. Lynch, C.W. Brown and R. Heidersbach, *Corrosion* **39** (1983) 357.
20. S. Shah, Corrosion'93, Paper 361, NACE International (1993).
21. J.A. Dougherty and B. Alink, *in* 'Proceedings of the 8th European Symposium on Corrosion Inhibitors (8 SEIC)', Vol. 10, Ferrara, Italy (1995), p. 1203.
22. S. Music, M. Gotic and S. Popovic, *J. Mater. Sci.* **28** (1993) 5744.
23. K.D. Efird, E.J. Wright, J.A. Boros and T.G. Hailey, *Corrosion* **49** (1993) 992.
24. R. De Marco, W.H. Durnie, A. Jefferson and B.J. Kinsella, *Corrosion* **57** (2001) 9.
25. K. Nakanishi and P.H. Solomon, 'Infrared Absorption Spectroscopy' (Holden Day, San Francisco, 1977).